Progress In Electromagnetics Research Letters, Vol. 40, 39–48, 2013

A WIDEBAND DIFFERENTIAL BANDPASS FILTER BASED ON T-SHAPED STUBS AND SINGLE RING RESONATOR

Hui Wang*, Wei Kang, Guo Yang, and Wen Wu

Ministerial Key Laboratory of JGMT, Nanjing University of Science and Technology, Nanjing 210094, China

Abstract—A wideband differential bandpass filter (BPF) with differential mode passband and common mode suppression is proposed and implemented on microstrip lines for wideband application in this letter. The initial BPF is similar to a single ring resonator with two unequal feed lines which have 180° separation and T-shaped stubs are loaded on the ring resonator to form an improved one for better performances. The lengths and widths of these stubs can be adjusted to produce a highly selectivity under the differential mode and improved attenuation under the common mode. This simple, compact structure is easy for construct without any coupling structure. Finally, a microstrip differential wideband BPF is designed, simulated, fabricated, and measured. The presented differential BPF has a 3-dB fractional bandwidth (FBW) of 38% for the differential mode and insertion loss greater than 17 dB for common mode. Good agreement between simulated and measured results is obtained.

1. INTRODUCTION

Balanced circuits are essential in building a modern communication system. Recently, under the trend of system-on-chip, it requires the integration of RF and analog circuits onto the digital baseband processor, thus the problem of interference and crosstalk from substrate coupling between components is getting more and more serious. For balanced circuits, differential filters with the advantages of high immunity to the environmental noises, good dynamic range, and low electromagnetic interference (EMI) are extremely important. These

Received 15 March 2013, Accepted 3 May 2013, Scheduled 8 May 2013

* Corresponding author: Hui Wang (w_h5300@sina.com).

filters should be able to produce the desired differential-mode frequency responses and reduce the common-mode signal interference at the same time, which is essential in increasing the signal-to-noise-ratio (SNR) in the receiver and improving the efficiency of the dipole antenna in the transmitter. In recent years, lots of structures have been demonstrated for differential bandpass filter (BPF) design, which are fabricated with single band, dual bands, wide band and improved common-mode suppression characteristics [1–14]. In [1], a novel ultra-wideband (UWB) differential filter is presented based on double-sided parallel-strip lines. In [2, 3], differential-mode UWB BPFs are fabricated with multiple stages branch-line. Theory and applications by means of complementary split ring resonators are discussed in [4, 5] for common-mode suppression in microstrip differential lines while both microstrip and defected ground structures (DGS) are utilized in [6, 7]. In [8, 9], many kinds of coupled structures are used for balanced filters applications. In [10, 11], balanced coupled-resonator BPFs with common-mode suppression and stopband extension are constructed based on stepped-impedance resonators and in [12, 13], various types of full differential bandpass filters are designed and fabricated. In [14], a new technique for realizing a fully differential filter using an operational amplifier (op amp) without common-mode feedback (CMFB) is presented.

In this letter, a wideband differential bandpass filter (BPF) with differential mode passband and common mode suppression is proposed and implemented on microstrip lines for wideband application. The initial BPF is similar to a single ring resonator with two unequal feed lines which have 180° separation and its improved one is formed by loading the T-shaped stubs on the ring for better performances. This structure is very simple, compact and easy for construct without any coupling structure. With the adoption of the 180° swap structure, the proposed filter presents a perfect electric conductor wall under common mode excitation and a perfect magnetic conductor wall under differential mode excitation along the symmetric line of the ring resonator. Thus, differential wideband BPF and common mode suppression can be obtained. The improved one is formed by loading the T-shaped stubs on the ring for better performances. Finally, a microstrip differential wideband BPF is designed, simulated, fabricated, and measured. The presented differential BPF has a 3-dB fractional bandwidth (FBW) of 38% for the differential mode and the common mode suppression is greater than 17 dB. Good agreement between simulations and measurements is obtained.

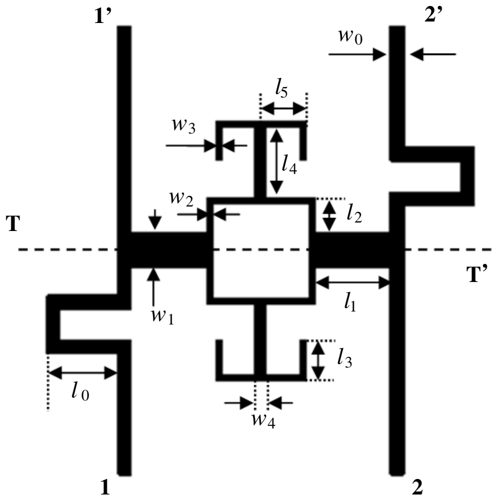

Figure 1. Configuration of the proposed wideband differential BPF.

2. ANALYSIS AND DESIGN

As depicted in Fig. 1, a wideband differential BPF with pairs of unequal feed lines, single ring resonator and T-shaped stubs is proposed. These unequal feed lines have 180° phase separation, which can be utilized to realize conversion between differential-mode and common-mode. If the input ports (ports 1 and 1′) are excited by differential-mode signals, the out-of-phase signals will be converted to in-phase signals when they pass through the 180° swap structure, then a virtual open appears at the symmetrical line T-T′ and a wideband BPF is constructed. Similarly, a virtual short appears at T-T′ when in-phase signals of ports 1 and 1′ are converted to out-of-phase and signals will be reflected to realize common-mode suppression. Then, the circuit schemes of common-mode and differential-mode can be obtained as shown in Fig. 2.

Figure 2 shows the equivalent half circuits of common- and differential-mode of the differential BPF. For the common-mode circuit in Fig. 2(a), signals will be reflected at the center short circuit point and common-mode suppression is obtained. As for the differential-mode circuit as shown in Fig. 2(b), it can be analyzed in even-odd-mode theory. T-shaped stubs have been loaded in some other circuits to improve the performances [15–21]. The presented T-shaped can be used in microstrip circuits to crate dual controllable transmission zeros for sharper skirt and some other better performances.

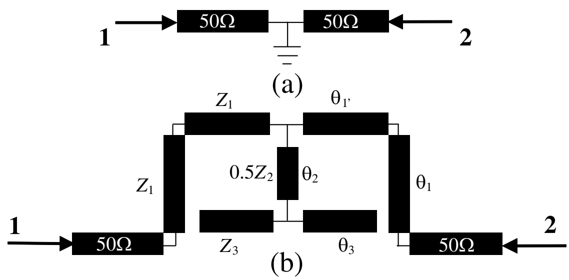

Figure 2. Equivalent half circuit of the proposed wideband differential BPF. (a) Common-mode equivalent half circuit. (b) Differential-mode equivalent half circuit.

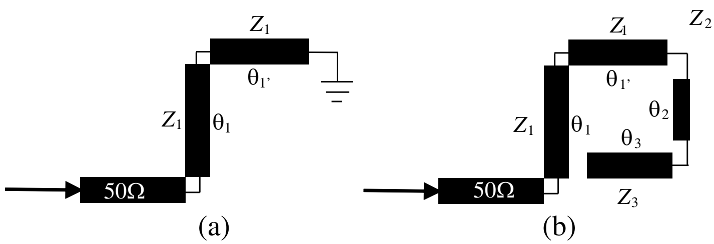

Figure 3. (a) Odd- and (b) even-mode equivalent circuits of the differential-mode half circuits of the BPF.

The transmission-line model of the differential-mode is shown in Fig. 3 [22], in which Fig. 3(a) presents its odd-mode circuit and (b) represents its even-mode circuit. For conventional denotation, the characteristic impedances of the stubs are Z_1, Z_2, and Z_3 while their electric lengths are θ_1, θ_1', θ_2, and θ_3, respectively.

For the odd-mode circuit in Fig. 3(a), the odd-mode input admittance Y_{odd} can be expressed as

$$Y_{\text{odd}} = -jY_1 \cot(\theta + \theta') \tag{1}$$

If $Y_{odd} = 0$, we can drive the resonance condition to determine the odd-mode resonant frequency. Fig. 4 plots the odd-mode resonant frequencies versus $\theta_x + \theta_x'$. Obviously, one transmission pole f_0 is located at $\theta_x + \theta_x' = 90\,\text{deg}$.

For the even-mode equivalent circuit of the differential-mode half circuit shown in Fig. 3(b), the even-mode input admittance Y_{even} is written as

$$Y_{\text{even}} = Y_1 \frac{Y_L + jY_1 \tan(\theta_1 + \theta_1')}{Y_1 + jY_L \tan(\theta_1 + \theta_1')} \tag{2}$$

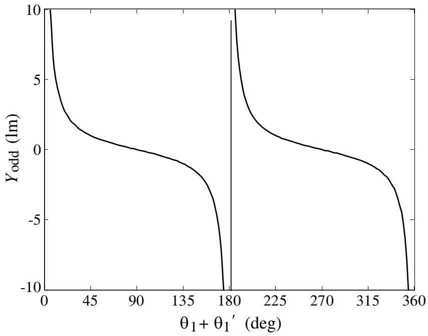

Figure 4. Odd-mode input admittance versus $\theta_1 + \theta_1'$.

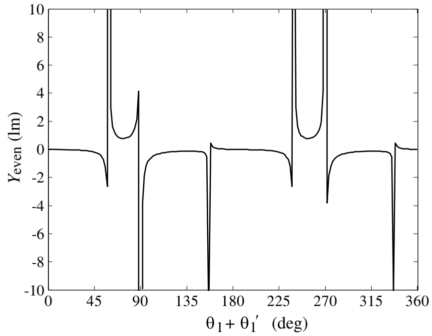

Figure 5. Even-mode input admittance versus $\theta_1 + \theta_1'$.

where

$$Y_L = jY_2 \frac{Y_3 + Y_2 \tan\theta_2 \cot\theta_3}{Y_3 \tan\theta_2 - Y_2 \cot\theta_3} \tag{3}$$

If $Y_{even} = 0$, the even-mode resonant frequencies can be determined. Thus, another two resonant frequencies f_1 and f_2 of even-mode can be obtained as

$$\theta_{e1} = \arctan\left(\sqrt{\frac{Y_1 - Y_2 + Y_3}{Y_1}}\right) \tag{4a}$$

$$\theta_{e2} = -\arctan\left(\sqrt{\frac{Y_1 - Y_2 + Y_3}{Y_1}}\right) \tag{4b}$$

Figure 5 plots the even-mode input admittance versus $\theta_x + \theta_x'$. Obviously, two transmission poles f_1 and f_2 are located at the sides of f_0.

The even-mode resonant frequencies spectrum versus Z_L/Z_1 is shown in Fig. 6. The two transmission poles f_1 and f_2 can be adjusted by changing the characteristic impedance Z_L (Z_2 and Z_3), thus the FBW of this filter can be controlled within a wide range.

To verify our discussion, a differential wideband filter is fabricated and measured. The configuration of the proposed differential wideband BPF is shown in Fig. 1. The filter is manufactured on RT/Duroid Rogers 4003 substrate with a relative permittivity of 3.38 and loss tangent of 0.0027, with a height of 0.508 mm. The photograph of the fabricated differential wideband BPF is shown in Fig. 7.

3. RESULTS AND DISCUSSION

Based on the above discussions and the theoretical analysis in Section 2, the final parameters for the differential filter with unequal feed lines are $Z_0 = 50\,\Omega$, $Z_1 = 80\,\Omega$, $Z_2 = 110\,\Omega$, and $Z_3 = 80\,\Omega$. The final structure parameters for the differential wideband BPF are $w_1 = 3.1\,\text{mm}$, $w_2 = 0.5\,\text{mm}$, $w_3 = 0.5\,\text{mm}$, $w_4 = 1.0\,\text{mm}$, $l_1 = 6.8\,\text{mm}$, $l_2 = 3.2\,\text{mm}$, $l_3 = 3.5\,\text{mm}$, $l_4 = 6.3\,\text{mm}$, and $l_5 = 4.0\,\text{mm}$.

To provide a simple figure-of-merit for characterizing the implement differential filter, the common-mode rejection ratio (CMRR) can be defined by

$$\text{CMRR} = 20\log\frac{\left|S_{21}^{dd}\right|}{\left|S_{21}^{cc}\right|} \tag{5}$$

The value of the CMRR may be used to quantitatively discuss the degree of resemblance between the implemented differential filter.

The simulated and measured results of S_{21}^{cc}, S_{21}^{dd}, S_{11}^{cc}, and S_{11}^{dd} for the proposed wideband differential BPF are shown in Figs. 8(a) and (b). Meanwhile, the CMRR provides an important figure-of-merit for a meaningful characterization of differential filters. Fig. 8(c) shows the simulated and measured responses of CMRR for the implemented differential filter based on unequal feed lines, T-shaped stubs and single ring resonator. Specifically, the filter has a maximum CMRR of more than 45 dB at the center frequency of the filter with all CMRR values above 17 dB between the 3-dB passband. The simulated results and measured results agree well with each other.

To clarify the proposed wideband differential BPF design, the design procedure can be summarized as follows:

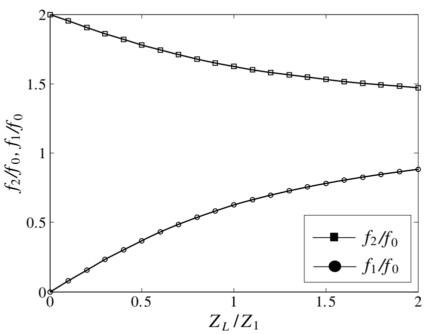

Figure 6. Even-mode resonant frequencies spectrum normalized with respect to f_0.

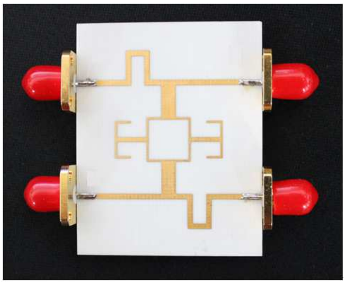

Figure 7. Photograph of the proposed filter.

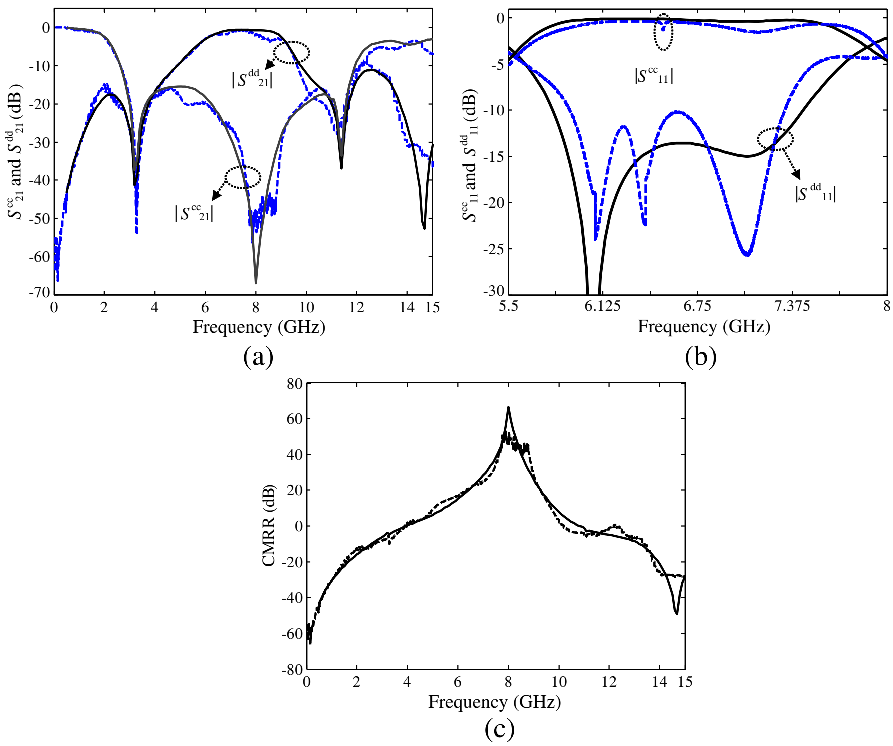

Figure 8. Simulated (solid line) and measured (dashed line) results of (a) S_{21}^{cc} and S_{21}^{dd}, (b) S_{11}^{cc} and S_{11}^{dd}, and (c) CMRR of the proposed differential filter.

1) The common mode suppression can be obtained easily using this filter structure due to the equivalent half circuit of common-mode equivalent half circuit as shown in Fig. 2(a).

2) The center frequency of differential mode can be determined by the electrical length of the ring resonator and the loaded T-shaped stubs, as analyzed in Equation (1).

3) Varied characteristic impedances of Z_1, Z_2, and Z_3 can be used to control the bandwidth of differential mode for the proposed wideband differential BPF, as shown in Fig. 6 and Equation (4).

4) The final dimensions can be obtained by using some microwave simulators although the open ends and cross sections will affect the practical electrical lengths of the resonator.

4. CONCLUSION

A wideband differential bandpass filter (BPF) with differential mode passband and common mode suppression is proposed and implemented on microstrip lines for wideband application. With the help of loaded T-shaped stubs, the performances of the filter are improved rather than the initial BPF which is similar to a single ring resonator with two unequal feed lines which have 180° separation. The presented differential BPF has a 3-dB fractional bandwidth (FBW) of 38% for the differential mode and larger than 17 dB common mode suppression. Good agreement between simulated and measured results is obtained. This simple, compact, and low cost structure will be very useful for differential communication systems.

ACKNOWLEDGMENT

The authors would like to express their great appreciate to editors and reviews for their valuable comments and suggestions.

REFERENCES

1. Wang, X. H. Q. Xue, and W. W. Choi, "A novel ultra-wideband differential filter based on double-sided parallel-strip line," *IEEE Microw. Wireless Compon. Lett.*, Vol. 20, No. 8, 471–473, 2010.
2. Lim, T. B. and L. Zhu, "Differential-mode ultra-wideband bandpass filter on microstrip line," *Electron. Lett.*, Vol. 45, No. 22, 1124–1125, 2009.
3. Lim, T. B. and L. Zhu, "Highly selective differential-mode wideband bandpass filter for UWB application," *IEEE Microw. Wireless Compon. Lett.*, Vol. 21, No. 3, 133–135, 2011.
4. Naqui, J., A. F. Prieto, M. D. Sindreu, F. Mesa, J. Matrel, F. Medina, and F. Martin, "Common-mode suppression in microstrip differential lines by means of complementary split ring resonators: theory and applications," *IEEE Trans. on Microwave Theory & Tech.*, Vol. 60, No. 10, 3023–3034, 2012.
5. Lim, T. B. and L. Zhu, "A differential-mode wideband bandpass filter on microstrip line for UWB application," *IEEE Microw. Wireless Compon. Lett.*, Vol. 19, No. 10, 632–634, 2009.
6. Shi, S. Y., W. W. Choi, W. Q. Che, K. W. Tam, and Q. Xue, "Ultra-wideband differential bandpass filter with narrow notched band and improved common-mode suppression by DGS," *IEEE Microw. Wireless Compon. Lett.*, Vol. 22, No. 4, 185–187, 2012.

7. Zhu, H. T., W. J. Feng, W. Q. Che, and Q. Xue, "Ultra-wideband differential bandpass filter based on transversal signal-interference concept," *Electron. Lett.*, Vol. 47, No. 18, 1033–1035, 2011.
8. Wu, C. H., C. H. Wang, and C. H. Chen, "Novel balanced coupled-line bandpass filters with common-mode noise suppression," *IEEE Trans. on Microwave Theory & Tech.*, Vol. 55, No. 2, 287–295, 2007.
9. Wu, X. H. and Q. X. Chu, "Compact differential ultra-wideband bandpass filter with common-mode suppression," *IEEE Microw. Wireless Compon. Lett.*, Vol. 22, No. 9, 456–458, 2012.
10. Shi, J. and Q. Xue, "Dual-band and wide-stopband single-band balanced bandpass filters with high selectivity and common-mode suppression," *IEEE Trans. on Microwave Theory & Tech.*, Vol. 58, No. 8, 2204–2212, 2010.
11. Lim, S. C. and C. Y, Yeh, "Stopband-extended balanced filters using both 1/4 and 1/2 SIRs with common-mode suppression and improved passband selectivity," *Progress In Electromagnetics Research*, Vol. 128, 215–228, 2012.
12. Wu, S. M., C. T. Kuo, and C. H. Chen, "Very compact full differential bandpass filter with transformer integrated using integrated passive device technology," *Progress In Electromagnetics Research Letters*, Vol. 113, 251–267, 2011.
13. Wu, S. M., C. T. Kuo, P. Y. Lyu, Y. L. Shen, and C. I. Chien, "Miniaturization design of full differential bandpass filter with coupled resonators using embedded passive device technology," *Progress In Electromagnetics Research Letters*, Vol. 121, 365–379, 2011.
14. Nicollini, G., F. Moretti, and M. Conti, "High frequency fully differential filter using operation amplifiers without common-mode feedback," *IEEE J. Solid-State Circuits*, Vol. 24, No. 3, 803–813, 1989.
15. Wang, H., W. Kang, C. Miao, and W. Wu, "Cross-shaped UWB bandpass filter with sharp skirt and notched band," *Electron. Lett.*, Vol. 48, No. 2, 96–97, 2012.
16. Feng, W. J., W. Q. Che, and Q. Xue, "Compact ultra-wideband bandpass filter implemented with stepped impedance resonators and T-shaped line," *International Conference on Micro. Millimeter Wave Tech., (ICMMT)*, 44–47, 2010.
17. Liu, G. Q., L. S. Wu, and W. Y. Yin, "A compact microstrip rat-race coupler with modified lange and T-shaped arms," *Progress In Electromagnetics Research Letters*, Vol. 115, 509–523, 2011.

18. Xie, J.-J., Y.-Z. Yin, S.-L. Pan, and L. Sun, "A novel circular slot antenna with two pairs of T-shaped slots for WLAN/WiMAX applications," *Progress In Electromagnetics Research Letters*, Vol. 32, 49–57, 2012.
19. Chen, L.-N., Y.-C. Jiao, Z. Zhang, F.-S. Zhang, and Y.-Y. Chen, "Miniaturized dual-mode substrate integrated waveguide (SIW) band-pass filters loaded by double/single T-shaped structures," *Progress In Electromagnetics Research Letters*, Vol. 29, 65–74, 2012.
20. Kang, L., Y.-Z. Yin, S.-T. Fan, and S.-J. Wei, "A novel rectangular slot antenna with embedded self-similar T-shaped strips for WLAN applications," *Progress In Electromagnetics Research Letters*, Vol. 15, 19–26, 2010.
21. Li, J.-F. and Q.-X. Chu, "Proximity-FED MIMO antenna with two printed IFAS and a wideband T-shaped neutralization line," *Progress In Electromagnetics Research M*, Vol. 21, 279–294, 2011.
22. Reed, J. and G. J. Wheeler, "A method of analysis of symmetrical four-port networks," *IRE Trans. on Microwave Theory & Tech.*, Vol. 4, No. 4, 246–252, 1956.